JCI The Journal of Clinical Investigation

AAV8-vectored suprachoroidal gene transfer produces widespread ocular transgene expression

Kun Ding, … , Olivier Danos, Peter A. Campochiaro

J Clin Invest. 2019. https://doi.org/10.1172/JCI129085.

Research Article Ophthalmology

Graphical abstract

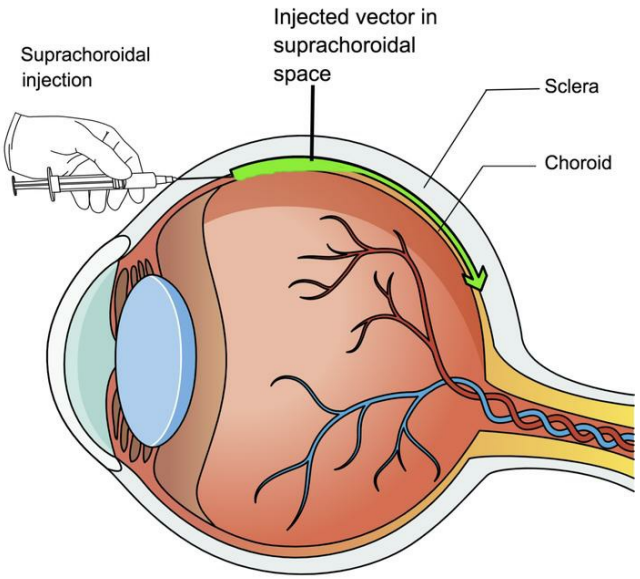

Find the latest version:

https://jci.me/129085/pdf

AAV8-vectored suprachoroidal gene transfer produces widespread ocular transgene expression

Kun Ding,[1] Jikui Shen,[1] Zibran Hafiz,[1] Sean F. Hackett,[1] Raquel Lima e Silva,[1] Mahmood Khan,[1] Valeria E. Lorenc,[1] Daiqin Chen,[1] Rishi Chadha,[1] Minie Zhang,[1] Sherri Van Everen,[2] Nicholas Buss,[2] Michele Fiscella,[2] Olivier Danos,[2] and Peter A. Campochiaro[1]

[1]Departments of Ophthalmology and Neuroscience, The Wilmer Eye Institute, Johns Hopkins University School of Medicine, Baltimore, Maryland, USA. [2]REGENXBIO Inc., Rockville, Maryland, USA.

There has been great progress in ocular gene therapy, but delivery of viral vectors to the retinal pigmented epithelium (RPE) and retina can be challenging. Subretinal injection, the preferred route of delivery for most applications, requires a surgical procedure that has risks. Herein we report a novel gene therapy delivery approach, suprachoroidal injection of AAV8 vectors, which is less invasive and could be done in an outpatient setting. Two weeks after suprachoroidal injection of AAV8.GFP in rats, GFP fluorescence covered 18.9% of RPE flat mounts and extended entirely around sagittal and transverse sections in RPE and photoreceptors. After 2 suprachoroidal injections of AAV8.GFP, GFP fluorescence covered 30.5% of RPE flat mounts. Similarly, widespread expression of GFP occurred in nonhuman primate and pig eyes after suprachoroidal injection of AAV8. GFP. Compared with subretinal injection in rats of RGX-314, an AAV8 vector expressing an anti-VEGF Fab, suprachoroidal injection of the same dose of RGX-314 resulted in similar expression of anti-VEGF Fab and similar suppression of VEGF-induced vascular leakage. Suprachoroidal AAV8 vector injection provides a noninvasive outpatient procedure to obtain widespread transgene expression in retina and RPE.

Introduction

Leber congenital amaurosis (LCA) is a group of diseases in which severe visual disability starts early in life. In a subgroup of patients with LCA due to a mutation in the *RPE65* gene, subretinal injection of an AAV2 vector carrying the WT *RPE65* gene resulted in improved mobility (1–3). The recent approval of this treatment by the Food and Drug Administration represents important validation of current and future potential of ocular gene therapy. Subretinal delivery of the *RPE65* gene was well-tolerated in most patients and the safety and tolerability of subretinal injection of viral vectors has been well-documented in other trials, particularly for sustained expression of antiangiogenic proteins where there is no need to detach the fovea (4). However, despite the overall benefit for the LCA study population, there were serious procedure-related complications in some study patients, including endophthalmitis, macular hole, and reduced visual acuity (5, 6). Any intraocular injection or procedure can result in endophthalmitis, but the longer and more involved a procedure, the greater the risk. Subretinal injections separate the photoreceptors from the retinal pigmented epithelium (RPE), which can compromise photoreceptors in a normal eye but may be particularly deleterious in an eye with photoreceptors damaged from an inherited retinal degeneration (3). Eyes with retinal degeneration also have subretinal fibrosis, which increases retinal-RPE adherence necessitating high infusion pressure to create a subretinal bleb. Since the fovea is the thinnest part of the macula, pressurized subretinal fluid may escape through the fovea, creating a macular hole, which may reduce vision. In addition, macular hole formation allows vector to escape into the vitreous cavity, reducing transduction efficacy. After subretinal vector injection, transfection occurs almost exclusively within the region of the bleb (the region where the photoreceptors and RPE are separated by the vector-containing fluid). The size and location of the bleb is critical but are not always easy to control because the path of least resistance, which determines the direction a bleb spreads, is not predictable from inspection of the retina at the time of surgery. Sometimes a bleb extends out symmetrically from a subretinal injection site, resulting in a circle, and sometimes it spreads asymmetrically to the retinal periphery in one direction, failing to involve an area of posterior retina that was targeted. A bleb may also extend more along the z axis than the x or y axes, resulting in a high bleb involving a relatively small area of retina and RPE. This unpredictability can be a source of variability in location and amount of transgene expression, resulting in variable outcomes that may be poor in some patients. Multiple subretinal injections

Authorship note: KD and JS contributed equally to the work.
Conflict of interest: These arrangements have been reviewed and approved by the Johns Hopkins University in accordance with its conflict-of-interest policies. PAC is an investigator for and has received grants from REGENXBIO Inc., Alimera Sciences Inc., Clearside Biomedical Inc., Sanofi Genzyme, Oxford Biomedica, and Regeneron Pharmaceuticals Inc.; he is a consultant for and has received honoraria and grants from Allergan Inc. and AsclepiX; he serves on the advisory board, is an investigator for, and has received honoraria and grants from Aerpio Pharmaceuticals and Genentech/Roche Inc.; he serves on the advisory board and has received honoraria from Applied Genetic Technologies Corporation, Exonate Ltd., and Merck & Co Inc.; he is a consultant for and has received honoraria from Astellas Pharma Inc. and Novartis Pharmaceuticals Corporation; he serves on the advisory board, is an investigator for, and has received a grant and equity from Allegro; he is a consultant for and cofounder of and has received honoraria, equity, and grants from Graybug Vision; he is a consultant and investigator for and has received honoraria and grants from RXI Pharmaceuticals. SVE, NB, MF, and OD are employees of REGENXBIO Inc.
Copyright: © 2019, American Society for Clinical Investigation.
Submitted: March 26, 2019; **Accepted:** August 7, 2019; **Published:** October 7, 2019.
Reference information: *J Clin Invest*. https://doi.org/10.1172/JCI129085.

in different locations may help to expose targeted areas of retina and RPE to vector, but increase the risk of complications.

Suprachoroidal injection has recently been demonstrated to provide a new route for ocular drug delivery. The suprachoroidal space is a potential space along the inner surface of the sclera that can be expanded by injection of fluid just inside the sclera. The development of microneedles with a length that approximates the thickness of the sclera has facilitated suprachoroidal injections (7), but suprachoroidal injections can also be done using standard needles. Fluorescently labeled particles injected near the limbus flow circumferentially around the eye, resulting in a broad area of exposure (8). Most small molecules have a half-life of a few hours in the suprachoroidal space, but lipophilic molecules such as triamcinolone acetonide form precipitates that dissolve slowly, providing sustained delivery to the retina (9, 10). Clinical trials have demonstrated prolonged improvement in macular edema in multiple disease processes after suprachoroidal injection of triamcinolone acetonide (11, 12). In this study, we investigated the potential value of suprachoroidal injection of AAV8 vectors for ocular gene transfer.

Results

Suprachoroidal injection of AAV8.GFP in rats results in GFP expression in RPE and photoreceptors throughout a large portion of the eye. The suprachoroid is a potential space between the choroid and the sclera that can be expanded by injection of fluid. Immediately after suprachoroidal injection of 3 μL India ink in a Brown Norway rat, the choroid was thickened and filled with ink on the side of the eye the injection was done (Figure 1A). There was gradual tapering to normal thickness by about half way around the eye, but ink was present within the choroid and extended all the way to the ora serrata opposite the injection site. High magnification views (Figure 1A, insets) showed that the ink extended from the sclera to the basal surface of the retinal pigmented epithelium (RPE) but did not enter the RPE or retina. Two weeks after suprachoroidal injection 1 mm posterior to the limbus of 3 μL containing 2.85×10^{10} gene copies (GCs) of AAV8.GFP in Brown Norway rats, a representative horizontal section through the equator of the globe showed green fluorescence in the choroid, RPE, and outer retina extending around the entire circumference of the eye (Figure 1B). Unlike an ocular section, which due to magnification allows visualization of modest levels of fluorescence, only very strong fluorescence can be visualized on flat mounts. So it is not surprising that while fluorescence was seen around the entire circumference of the eye in the section shown in Figure 1B, fluorescence could only be visualized in the quadrant proximal to the injection site on a retinal flat mount, with no detectable fluorescence on the opposite side of the eye (Figure 1C). There was strong GFP fluorescence throughout a slightly larger area of RPE flat mounts (Figure 1D). High magnification views showed considerable heterogeneity of GFP fluorescence within hexagonal RPE cells with bi-lobed nuclei (Figure 1E). One and 2 weeks after suprachoroidal injection of 2.85×10^{10} GCs of AAV8.GFP, mean levels of GFP protein measured by ELISA in RPE/choroid and retinal homogenates were high, in the range of 100 ng/mg protein (Figure 1F). There was no detectable GFP in liver by ELISA, indicating that there was not enough vector entering the systemic circulation to transduce liver cells. Sagittal ocular sections (anterior to posterior) 2 weeks after injection showed that fluorescence corresponded well to immunohistochemical staining with an anti–GFP antibody (Figure 1, G–L). In the posterior retina on the injected side of the eye, there was strong GFP staining in the RPE and the majority of photoreceptor cell bodies, inner segments, and outer segments (Figure 1, G–I). At the equator on the opposite side of the eye, there was strong staining in RPE, but fewer photoreceptor cell bodies, inner segments, and outer segments had detectable staining (Figure 1, J–L).

A transverse section (injected side to opposite side) half way between the equator and the posterior pole 2 weeks after suprachoroidal injection of 2.85×10^{10} GCs of AAV8.GFP showed fluorescence in the RPE and outer retina that was strongest on the injected side of the eye (bottom), but that extended around to the opposite side (Figure 2, upper). High power views of the boxed regions showed immunohistochemical staining for GFP in RPE and photoreceptor cell bodies, inner segments, and outer segments. Compared with the 2 remote quadrants (Figure 2, A and B), GFP staining was stronger in the 2 quadrants closer to the injection site (Figure 2, C and D). There was good correspondence between GFP fluorescence and anti–GFP staining (Supplemental Figure 1; supplemental material available online with this article; https://doi.org/10.1172/JCI129085DS1). Interestingly, photoreceptor inner and outer segments contained substantial levels of GFP in all 4 locations, but there was less GFP within photoreceptor cell bodies in the remote locations. There was little GFP in cells of the inner retina (Figure 2, A and D). A transverse section half way between the equator and the posterior pole 2 weeks after subretinal injection of 2.85×10^{10} GCs of AAV8.GFP showed strong fluorescence in the outer retina and RPE on one side of the eye, but no detectable fluorescence on the opposite side of the eye (Figure 2, lower). Compared with the 2 remote quadrants which showed minimal immunohistochemical staining for GFP (Figure 2, E and F), there was strong staining for GFP in the 2 quadrants on the side of the injection (Figure 2, G and H).

Augmentation of GFP expression by a second suprachoroidal AAV8.GFP injection in rats. To evaluate if a second injection would increase transduction, rats (n = 21) had suprachoroidal injections of 2.85×10^{10} GCs of AAV8.GFP in both eyes and 3 days later had a second suprachoroidal injection of 2.85×10^{10} GCs on the opposite side of one eye. Fourteen days after the injection in both eyes and 11 days after the second injection in one eye, a representative RPE flat mount showed GFP fluorescence on one side for the single injection eye (Figure 3A) and strong fluorescence on both sides for the double injection eye (Figure 3B). The mean percentage of RPE flat mount coverage with strong GFP fluorescence was 18.9% in single injection eyes compared with 30.5% in eyes that received 2 injections (n = 6, P = 0.026). The remainder of the rats had measurement of GFP protein by ELISA in homogenates of RPE/choroid and retina. There was a significant increase in mean level of GFP protein per mg total protein in eyes that received 2 injections compared with those that receive a single injection (Figure 3C).

Suprachoroidal injection with AAV9.GFP, but not AAV2.GFP, provides GFP expression comparable to that seen with AAV8.GFP. Two weeks after suprachoroidal injection of 2.85×10^{10} GCs of AAV9.GFP, retinal flat mounts showed strong fluorescence in the quadrant in which the injection was done, with no detect-

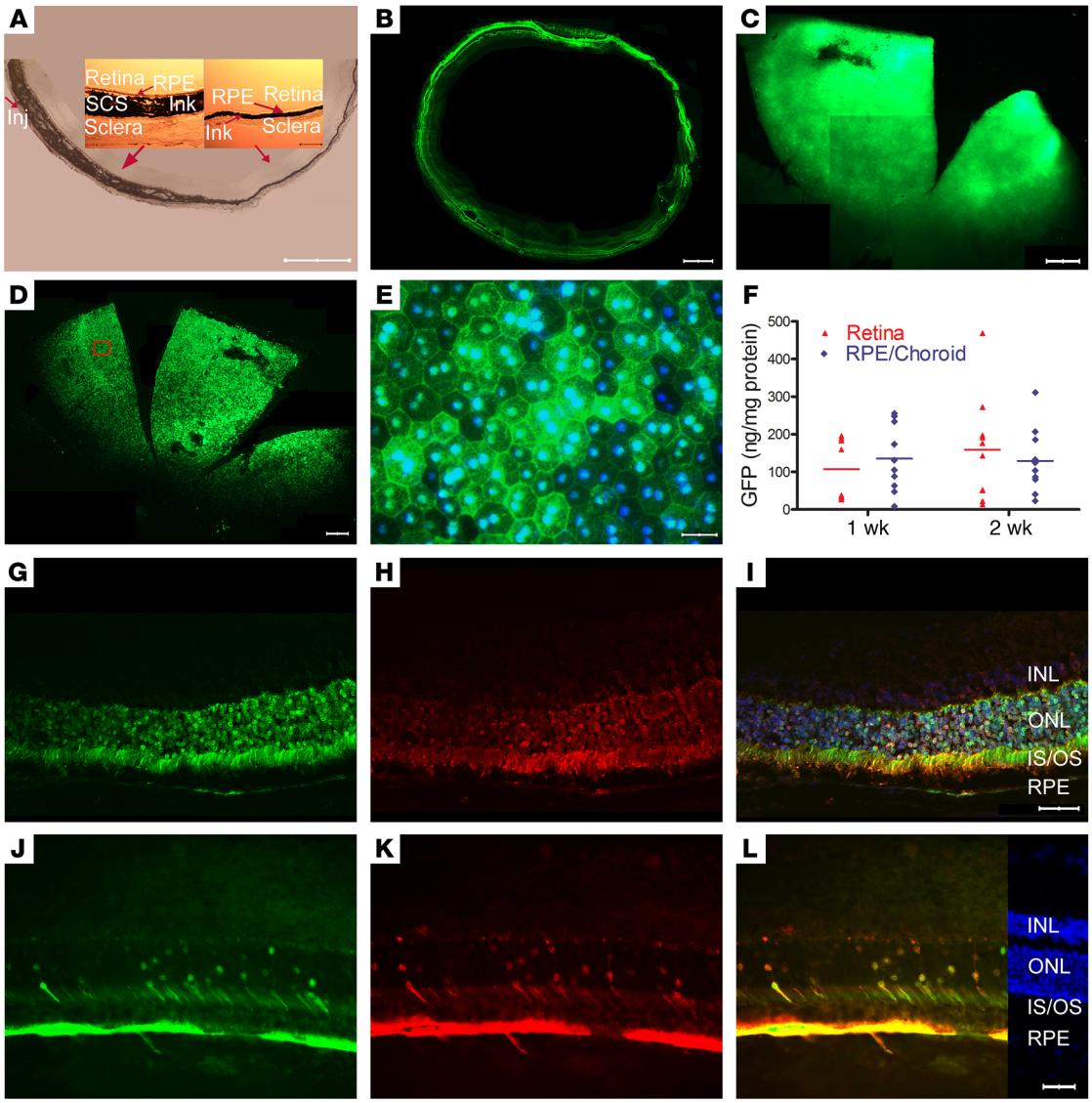

Figure 1. Widespread expression of GFP after suprachoroidal injection of AAV8.GFP in rats. (**A**) Immediately after suprachoroidal injection of India ink (3 μL) in rats, frozen sections showed increased choroidal thickness on the side of injection that tapered to normal, but ink extended completely around the eye. Scale bar: 1000 μm. High magnification showed ink from the sclera to the basal surface of the RPE (insets; scale bar: 100 μm). (**B**) Two weeks after suprachoroidal injection of 2.85×10^{10} GCs of AAV8.GFP, 10-μm horizontal frozen sections at the equator showed GFP in the retina and RPE extending around entire circumference of the eye. Scale bar: 500 μm. (**C**) A retinal flat mount showed high GFP expression in about one-fifth of the retina from anterior edge posteriorly nearly to the optic nerve. Scale bar: 500 μm. (**D**) There was GFP throughout about one-fifth of a RPE flat mount from the anterior edge posteriorly almost to the optic nerve. Scale bar: 500 μm. (**E**) Higher magnification of boxed region shows strong GFP fluorescence in some RPE cells and little fluorescence in others. Scale bar: 50 μm. (**F**) The mean ± SEM level of GFP measured by ELISA was high in retinal or RPE/choroid homogenates at 1 and 2 weeks after suprachoroidal injection ($n = 10$ for each group). Two weeks after vector injection, an ocular section through the posterior part of the eye near the optic nerve shows strong fluorescence in the RPE, photoreceptor cell bodies, inner segments, and outer segments (**G**). The same section immunohistochemically stained with anti-GFP antibody (**H**) and merged with the image in **G** shows that the fluorescence is due to GFP (**I**; scale bar: 50 μm). An ocular section from the equator of the eye on the side opposite the site of injection shows strong GFP expression in RPE but in a minority of photoreceptor cell bodies and inner segments (**J**–**L**; scale bars: 50 μm). INL, inner nuclear layer; ONL, outer nuclear layer; IS, photoreceptor inner segment; OS, photoreceptor outer segment; RPE, retinal pigmented epithelium.

able fluorescence on the opposite side of the eye (Supplemental Figure 2A). RPE/choroid flat mounts also showed strong GFP fluorescence in the quadrant in which the injection was done (Supplemental Figure 2B), and high magnification view of the boxed region showed heterogeneity of GFP fluorescence within RPE cells similar to that seen after AAV8.GFP injection (Supplemental Figure 2C). Two weeks after suprachoroidal injection of 2.0×10^{10} GCs of AAV2.GFP there was a small focal area of fluorescence limited to the far periphery of the retina (Supplemental Figure 2D) and RPE (Supplemental Figure 2E) near the injection site. A magnified view of the boxed region showed strong fluorescence in some RPE cells and weak fluorescence in others (Supplemental Figure 2F). An ocular section at the equator superiorly in an eye injected with AAV9.GFP showed GFP

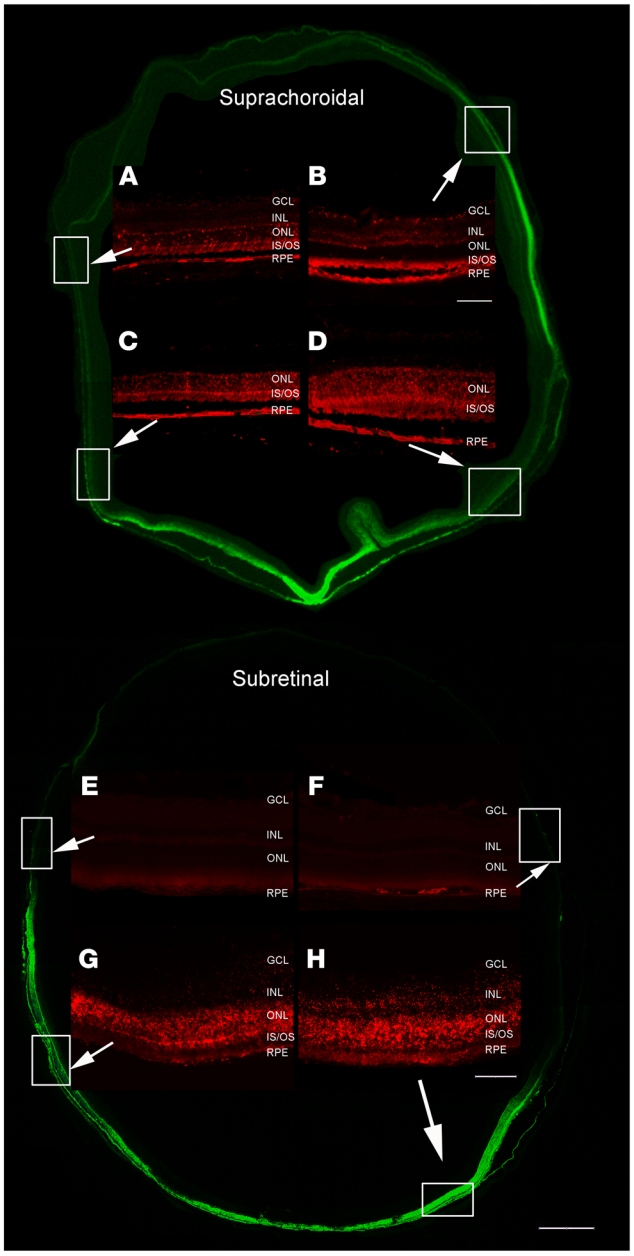

Figure 2. Expression of GFP throughout the posterior retina and RPE 2 weeks after suprachoroidal or subretinal injection of AAV8.GFP in rats. Two weeks after suprachoroidal injection of 2.85×10^{10} GCs of AAV8.GFP in rats, a transverse section showed more intense fluorescence in the retina on the side of the eye where the injection was performed (bottom), but was detectable around the entire circumference of the eye. The section was immunohistochemically stained with anti-GFP (red), and magnified views of the boxed regions on the side opposite the injection site (**A** and **B**) or on the same side (**C** and **D**) are shown. (**A**) In this region remote from the injection, there is strong GFP expression in some but not all RPE cells. Almost all photoreceptor inner segments (IS) and outer segments (OS) contain GFP, but few photoreceptor cell bodies in the outer nuclear layer (ONL). (**B**) In this second remote region, there are high levels of GFP in the RPE cells and photoreceptor IS and OS, but not cell bodies. Some cells in the inner nuclear layer (INL) and GCL contain GFP (**C** and **D**). In the 2 regions on the injected side of the eye, there are high levels of GFP in RPE cells and photoreceptor IS, OS, and cell bodies. There is a small artifactual retinal fold adjacent to the boxed area shown in **D**. Two weeks after subretinal injection of 2.85×10^{10} GCs of AAV8.GFP, there was strong GFP fluorescence and anti-GFP staining in RPE, photoreceptor IS, OS, and cell bodies in half of the eye where the retina had been detached by the vector (**G** and **H**), but not the other half (**E** and **F**). Scale bars: 100 μm for high power; 500 μm for low power.

in RPE, photoreceptor inner and outer segments, and some photoreceptor cell bodies (Supplemental Figure 2G). An ocular section from the periphery of the eye near the injection site in an eye injected with AAV2.GFP showed GFP in RPE cells (Supplemental Figure 2H).

Suprachoroidal injection of RGX-314 suppresses VEGF-induced vasodilation and vascular leakage. The above studies with AAV8.GFP show that suprachoroidal injections of AAV8 vectors can provide widespread transgene expression in the RPE/choroid and retina, but provide no information on potential biological effects. We therefore performed experiments with RGX-314, an AAV8 vector that expresses an anti–VEGF Fab that selectively binds human but not rat or mouse VEGF. Subretinal injection of RGX-314 strongly suppresses retinal and choroidal neovascularization (NV) in transgenic mice that express human VEGF in the retina (13). We are unable to perform suprachoroidal injections in mice due to the small size of the eye. Therefore, we tested the effects of RGX-314 in a rat model of human VEGF-induced leakage. Rats were given a suprachoroidal or a subretinal injection of 1.2×10^8 GCs of RXG-314 in one eye and vehicle in the fellow eye. We previously demonstrated that we could not visualize fluorescence in the retina after suprachoroidal injection of 2.85×10^{10} GCs of AAV8.GFP by photography using the same filters used for fluorescein angiography, but to avoid any possible concern, we used vehicle rather than GFP vector for controls in this part of the experiment. At 2 weeks after injection, rats were given an intravitreous injection of 100 ng recombinant human $VEGF_{165}$ (VEGF) in each eye. Twenty-four hours later, fundus photographs showed normal retinas and retinal vessels in eyes that had previously been given an injection of RGX-314, either by suprachoroidal route (Figure 4A) or subretinal route (Figure 4C). In contrast, fellow control eyes that had previously been given a suprachoroidal (Figure 4B) or subretinal (Figure 4D) injection of vehicle showed dilated, engorged vessels and in some cases hemorrhages (Figure 4B, arrow). Fluorescein angiograms showed retinal vessels with normal caliber and sharp margins in eyes given suprachoroidal (Figure 4E) or subretinal (Figure 4G) injection of RGX-314, while those given suprachoroidal (Figure 4F) or subretinal (Figure 4H) injection of vehicle showed dilated vessels with somewhat hazy margins. The findings 7 weeks after vector injection were similar to those seen 2 weeks after injection. Eyes that had been given suprachoroidal or subretinal injection of RGX-314 showed normal retinas and retinal vessels with normal caliber and sharp margins (Figure 4, I, K, M, O), while fellow eye controls that had been given suprachoroidal or subretinal injection of vehicle (Figure 4, J, L, N, P) showed retinal hemorrhages (Figure 4, J and L, arrows) and dilated retinal vessels with indistinct margins (an indication of leakage).

Serum albumin provides a widely used endogenous marker for vascular leakage in the retina (14–18). In naive WT rats, there is a relatively low level of albumin in the vitreous that varies little among different rats (Figure 4Q, naive). In rodent eyes given

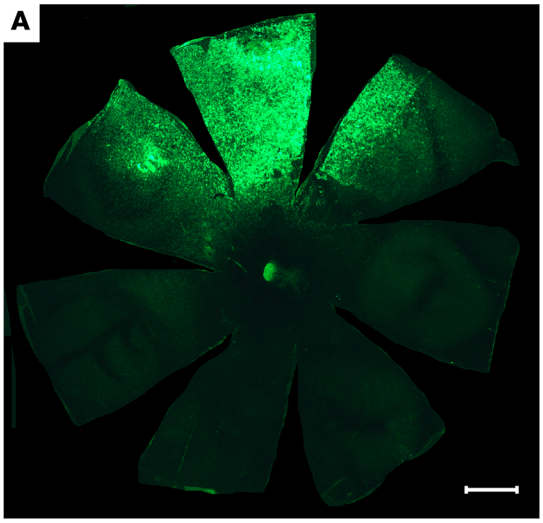

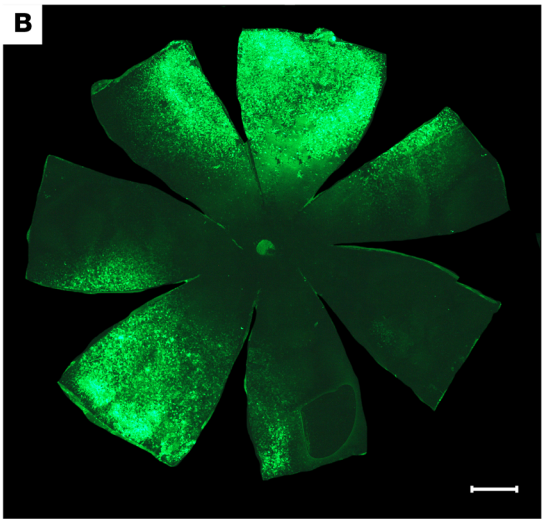

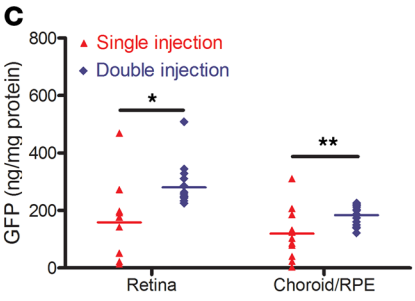

Figure 3. Increase in area and level of GFP expression after a second suprachoroidal injection of AAV8.GFP in rats. Brown Norway rats (n = 21) were given a 3 μL suprachoroidal injection containing 2.85 × 10^{10} GCs of AAV8.GFP vector superiorly in both eyes. Three days later, one eye was given an inferior 3 μL suprachoroidal injection containing 2.85 × 10^{10} GCs of AAV8.GFP and the other eye received no injection. After 11 days, RPE flat mounts showed high GFP fluorescence in 1 localized region of eyes that had received 1 injection (**A**) and in 2 regions of eyes that received 2 injections (**B**); scale bars: 1000 μm. The mean percentage of total RPE area that was fluorescent was significantly greater in eyes that received 2 injections (30.52%) compared with those that received 1 injection (18.85 %, n = 6, P = 0.026 by Mann-Whitney U test). (**C**) For the remaining 15 rats, 2 eyes in the single injection group had been traumatized and could not be used, but for the remainder, homogenates of RPE/choroid and retinas were used to measure total protein and then GFP protein was measured by ELISA. The mean (± SEM) level of GFP per mg protein was significantly higher in retinas and RPE/choroid from eyes that received 2 injections compared with those that received 1 injection. *P = 0.0008; **P = 0.005 by Mann-Whitney U test and unpaired t test.

an intravitreous injection of VEGF or in the eyes of rodents with retinal/choroidal vascular disease, albumin from serum leaks into the vitreous and the amount of albumin in the vitreous provides a quantitative assessment of excessive vascular permeability (19, 20). Twenty-four hours after intravitreous injection of 100 ng VEGF, eyes that had 2 or 7 weeks before been given suprachoroidal or subretinal injection of RGX-314 had significantly lower mean vitreous albumin than fellow eye controls that had been given suprachoroidal or subretinal injection of AAV8.GFP (Figure 4Q). AAV8.GFP was used as control in this portion of the experiment because it is a biochemically irrelevant vector, and visualization, which could be confounded by any GFP fluorescence if it were discernable, was not part of the assessment. The mean level of anti–VEGF Fab protein in retina and RPE/choroid was similarly high 2 and 7 weeks after suprachoroidal or subretinal injection of 1.2 × 10^8 GC, with no significant difference between the 2 routes of administration in either tissue at both time points (Figure 4R). Thus, the total amount of transgene expression is similar when the same amount of vector is injected into the suprachoroidal or subretinal space.

Suprachoroidal injection of AAV8.GFP in nonhuman primates and pigs. In order to evaluate suprachoroidal gene transfer in eyes closer in size and structure to human eyes, 3 rhesus monkeys and one Yorkshire pig were given a suprachoroidal injection of 50 μL containing 4.75 × 10^{11} GCs of AAV8.GFP in each eye. The monkeys showed no detectable neutralizing anti-AAV8 serum antibodies prior to injection. Twenty-one days after injection, serum titers for neutralizing anti-AAV8 serum antibodies was 1:256 in 2 monkeys and 1:512 in the third. Retinal and RPE/choroid flat mounts 21 days after injection were prepared and because the monkey eye is much larger than a rat eye, even at low magnification only a small portion of a flat mount can be captured in a single photographic image. A composite generated by stitching overlapping images together showed high GFP expression throughout approximately one-third of the retinal flat mount (Figure 5A). Higher magnification of the midperiphery of an RPE/choroid flat mount in the quadrant of the injection showed heterogeneity of GFP expression with some RPE cells showing strong fluorescence and others showing little or none (Figure 5B). Additional magnification showed the hexagonal shape of the RPE cells (Figure 5C). Lighter, more homogeneous fluorescence was seen in posterior RPE cells adjacent to the optic nerve (Figure 5, D and E). In contrast, the lower half of the RPE flat mount showed no detectable fluorescence, indicating that the fluorescence seen in the quadrants adjacent to the suprachoroidal injection of AAV8.GFP was due to GFP expression and not autofluorescence. Retinal flat mounts showed many fluorescent cells in the multilayered retina extending posteriorly to the cut edge of retina where it had been severed from the optic nerve (Figure 5F). Two weeks after a suprachoroidal injection of 50 μL containing 4.75 × 10^{11} GCs of AAV8.GFP in a Yorkshire pig, an

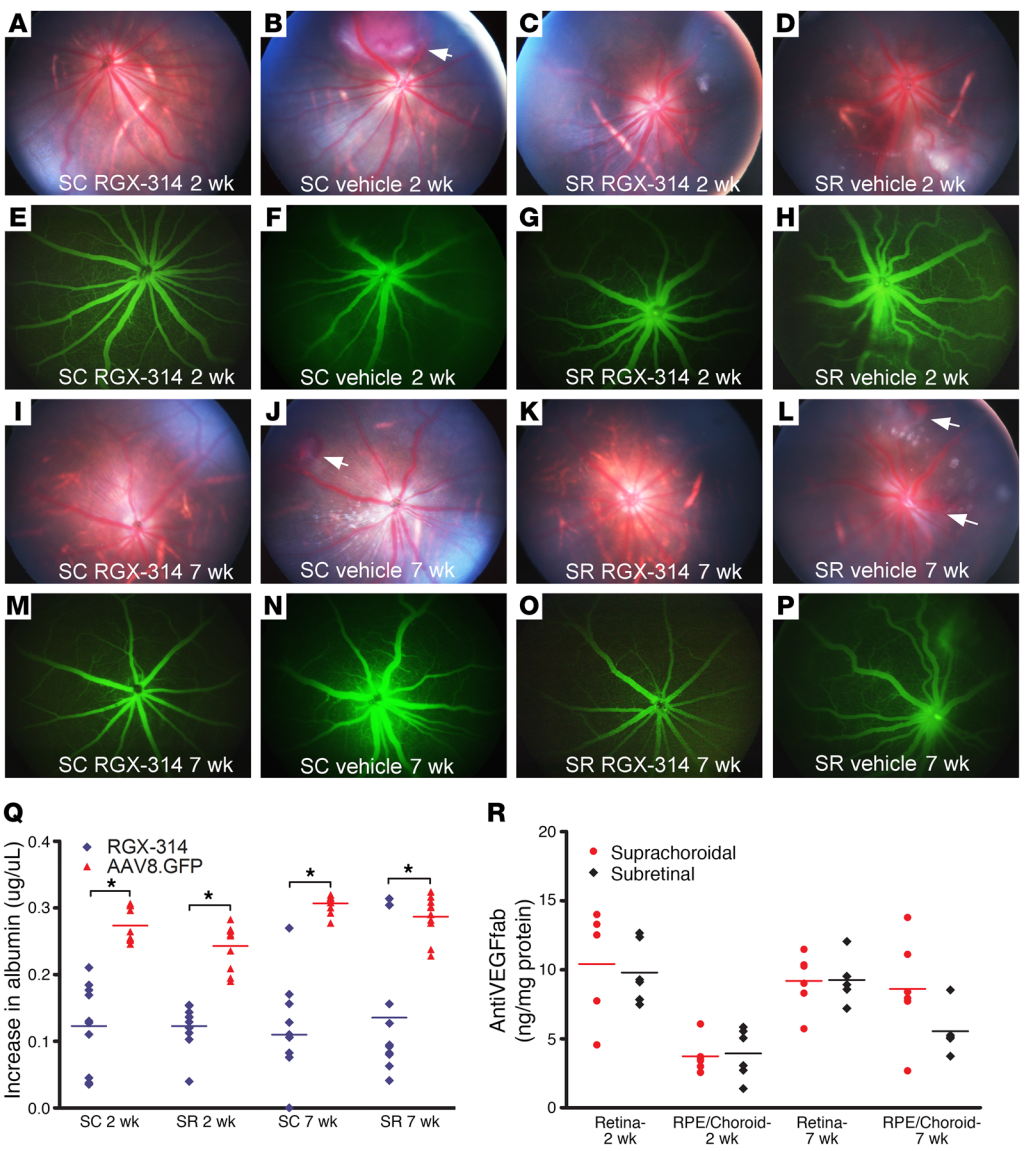

Figure 4. Suprachoroidal versus subretinal injection of RGX-314. Rats were given suprachoroidal (SC) or subretinal (SR) injection of 1.2×10^8 GCs of RGX-314 in one eye and SC or SR vehicle injection in the other eye. After 2 weeks, intravitreous VEGF (100 ng) was given and 24 hours later, fundus photographs showed normal retinas and retinal vessels in eyes given SC (**A**) or SR (**C**) injection of RGX-314, whereas SC (**B**) or SR (**D**) vehicle controls showed dilated, engorged vessels and hemorrhages (**B**, arrow). Fluorescein angiograms (FAs) showed normal caliber vessels with sharp margins in SC (**E**) or SR (**G**) RGX-314–injected eyes, whereas vehicle controls showed dilated vessels with blurred margins (**F** and **H**). Results were similar 7 weeks after vector injection. Twenty-four hours after VEGF (100 ng) injection, eyes that had been given SC (**I** and **M**) or SR (**K** and **O**) injection of RGX-314 showed normal retinal vessels with sharp margins in FAs, whereas vehicle controls showed dilated retinal vessels and hemorrhages (**J** and **L**, arrows), and hazy margins in FAs (**N** and **P**). (**Q**) Two or 7 weeks after SC or SR injection of RGX-314 or AAV8.GFP in the fellow eye, mean (± SEM) vitreous albumin measured by ELISA 24 hours after VEGF (100 ng) injection was significantly less in SC or SR RGX-314–injected eyes versus fellow eye controls ($n = 10$, $^*P < 0.03$ by unpaired t test). (**R**) Mean (± SEM) anti–VEGF Fab in the retina and RPE/choroid were high 2 or 7 weeks after RGX-314 injection with no significant difference between the SC and SR routes of injection at each time point ($n \geq 5$).

ocular section from posterior retina in the quadrant the injection was done showed colocalization of fluorescence and anti-GFP staining in RPE and photoreceptor inner and outer segments and cell bodies (Figure 5G). There was also a small region of GFP expression in the inner retina.

Discussion

The eye is a relatively confined space which is advantageous for gene transfer because only small amounts of vector are needed and exposure to the remainder of the body is limited. Two major applications for ocular gene transfer are delivery of WT genes to compensate for mutant genes that cause retinal degeneration and delivery of genes that provide sustained expression of therapeutic proteins; considerable progress has been made in both of these areas (1–4, 21–23). AAV vectors have emerged as the most widely used vectors for ocular gene transfer and 2 routes of delivery have been studied, intravitreous injection and subretinal injection. Intravitreous injection can be done in an outpatient

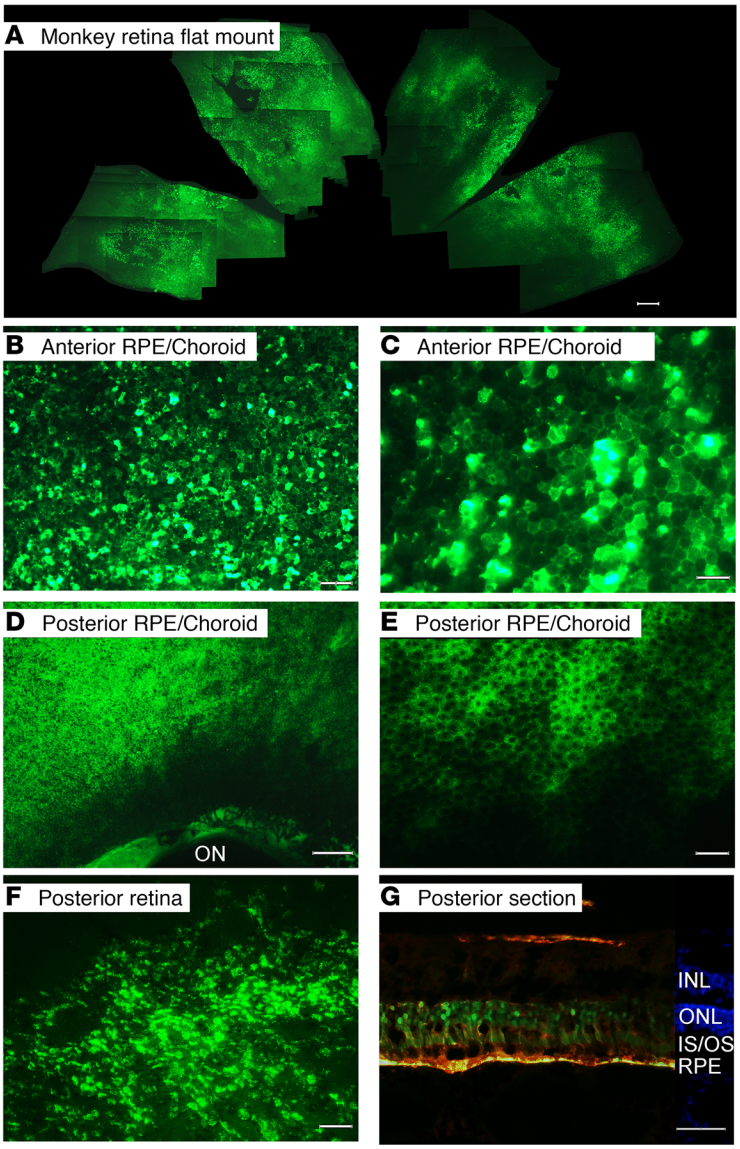

Figure 5. Widespread expression of GFP 3 weeks after suprachoroidal injection of AAV8.GFP in nonhuman primates or pigs. Rhesus monkeys were given a suprachoroidal injection of 50 μL containing 4.75×10^{11} GCs of AAV8.GFP and after 3 weeks flat mounts were examined by fluorescence microscopy. The flat mounts and sections from each of the eyes showed similar results and therefore representative images are shown. A collage was made from one eye by aligning areas of overlap. The collage shows strong expression of GFP throughout approximately one-third of the retinal flat mount (**A**; scale bar: 1000 μm). In a RPE flat mount, high magnification view of the mid-periphery in the quadrant of injection shows heterogeneity of GFP expression with intense fluorescence in some RPE cells and little or none in others (**B**; scale bar: 100 μm). A higher magnification view shows the hexagonal shape of RPE cells, some seen in negative relief (**C**; scale bar: 50 μm). Posteriorly there is less intense, but more uniform GFP expression in RPE cells extending almost to the border of the optic nerve (ON) which is outlined by fluorescence (**D**; scale bar: 250 μm). Higher magnification shows the hexagonally shaped RPE cells with GFP in the cytoplasm and the nuclei in negative relief (**E**; scale bar: 50 μm). Retinal flat mounts showed GFP expression in many cells of the multilayered retina extending posteriorly to the cut edge of retina where it had been severed from the optic nerve (**F**; scale bar: 50 μm). Two weeks after suprachoroidal injection of 50 μL containing 4.75×10^{11} GCs of AAV8.GFP in a pig, merged images from ocular sections showed colocalization of fluorescence and anti-GFP staining in RPE cells and photoreceptor inner and outer segments (**G**; scale bar: 50 μm). There is also some GFP expression in the inner retina.

clinic and exposes all cells lining the vitreous cavity to vector, but expression in the retina is limited to a small population of ganglion cells surrounding the fovea and transitional epithelium of the pars plana. This precludes intravitreous delivery for gene replacement in photoreceptors and severely compromises its use for long-term expression of therapeutic proteins. Subretinal injection of AAV vectors results in strong transgene expression in RPE and photoreceptors within the retinal detachment caused by the injection. This provides the ability to replace mutant genes in photoreceptors or RPE in the area of the detachment or strongly express soluble therapeutic proteins that can access the entire retina. The disadvantages of subretinal injection of vector are that (i) it requires going to the operating room and performing vitrectomy, which induces cataract in the majority of patients and is complicated by retinal detachment in a small percentage, (ii) gene delivery is limited to a relatively small area of the retina and RPE that borders the bleb, requiring prioritization of the most important region to be targeted for gene replacement and sacrificing the remainder of the retina and RPE, and (iii) since the fovea has the highest visual potential, it is high priority for gene replacement, but separation of already compromised photoreceptors and RPE by retinal detachment from subretinal injection of vector may cause permanent damage that reduces vision, providing a quandary (3). Direct comparison of subretinal and intravitreous injections of AAV8 reporter gene vectors in mice showed that 1 year after injection there was significant reduction in electroretinographic retinal function in eyes that had received a subretinal injection compared with those that had received an intravitreous injection (24).

In view of these limitations of currently used routes of administration, there have been attempts to improve them or identify alternative approaches. Peden et al. (25) performed a surgical procedure in rabbits in which a microcatheter was inserted into the suprachoroidal space and advanced posteriorly to the region of the optic nerve where self-complementary AAV5-smCVA-hGFP was injected, resulting in GFP expression in choroid, RPE, and retina. In this study, we have shown that AAV8 vectors can be injected into the suprachoroidal space without a surgical procedure or use of a microcatheter and cause widespread transgene expression throughout the RPE and photoreceptors of the eye. This has important advantages because it can be done in an outpatient setting like intravitreous injections, thereby avoiding the risks of a more invasive surgical procedure and the inconvenience of going to the operating room. It also eliminates the risks of separating photoreceptors from the RPE in the fovea. Compared with spread of vector in the subretinal space, there is much greater spread in the suprachoroidal space (Figure 1A), allowing expression throughout a larger area of RPE/choroid and retina (Figure 2). Fluorescence microscopy of retinal sections, the most sensitive way of visualiz-

ing GFP, showed expression extending around the entire circumference of the eye at the equator 2 weeks after a single suprachoroidal injection of 2.85×10^{10} GCs of AAV8.GFP in rats (Figure 1B). The GFP expression occurred predominantly in RPE and photoreceptors. Only high levels of GFP can be visualized by fluorescence microscopy of RPE or retinal flat mounts and approximately one-fifth of each showed high expression (Figure 1, C and D). The area of high GFP expression was increased by a second injection 3 days after the first. This suggests that, using multiple suprachoroidal injections of AAV8 vector, it would be possible to achieve high level expression throughout most or all of the RPE/choroid and photoreceptors. This could be achieved during a single clinic visit by performing suprachoroidal injections in each of the 4 quadrants of the eye, waiting for the intraocular pressure to normalize after each injection, or accelerating that normalization by anterior chamber taps.

Gene therapy is a potentially transformative treatment for relatively rare inherited retinal degenerations and therefore has tremendous potential for patients with that uncommon condition. Gene delivery of therapeutic proteins has the potential to revolutionize the management of millions of patients with common retinal and choroidal vascular diseases. VEGF is a critical stimulus in neovascular age-related macular degeneration (NVAMD), diabetic macular edema (DME), diabetic retinopathy, and macular edema secondary to retinal vein occlusion (RVO) (26). The current approach in each of these conditions is intravitreous injection of VEGF-neutralizing proteins, which reduce vascular leakage and improve vision, but these diseases are chronic with sustained overexpression of VEGF requiring frequent, repeated injections in most patients. It is difficult for patients and physicians to maintain the optimal injection frequency over many years so that in patients with NVAMD treated outside clinical trials, long-term visual outcomes are substantially worse than those reported in clinical trials (27–29). Gene transfer of expression constructs coding for a VEGF-neutralizing protein provides a good strategy to provide reliable, long-term suppression of chronically overexpressed VEGF. A clinical trial testing the effect of intravitreous injection of AAV2.sFLT01 showed detectable expression in some patients with NVAMD given the highest dose and suppressed leakage reducing the need for anti-VEGF injection in some patients, but was insufficient to provide stability in the majority of patients (23). In contrast, preclinical studies have shown reliable, high level expression of an antibody fragment that binds VEGF after subretinal injection of RGX-314 that resulted in impressive efficacy in models relevant to NVAMD (13), and this is currently being tested in a clinical trial (ClinicalTrials.gov, NCT03066258). In this study, we have demonstrated in rats that compared with subretinal injection of 1.2×10^8 GCs of RGX-314, suprachoroidal injection of the same amount of RGX-314 provided similar expression of anti–VEGF Fab and similar suppression of VEGF-induced vascular leakage.

We chose to use AAV8 vector for these proof-of-concept studies, because AAV8 efficiently transduces a wide variety of cell types and because our prior studies investigating subretinal injection of RGX-314 provided motivation for testing the potential of suprachoroidal injection of AAV8 vectors. To determine if the ability to strongly transduce photoreceptors and RPE after suprachoroidal injection was unique to AAV8, we performed brief comparative studies in rats with 2 other serotypes, AAV9 and AAV2. There was strong transduction of RPE and photoreceptors after suprachoroidal injection of AAV9.CB7.GFP, similar to AAV8.CB7.GFP, but poor transduction after suprachoroidal injection of AAV2.CMV.GFP. This suggests that there are differences among AAV serotypes with regard to transduction efficiency after suprachoroidal injection, and that AAV2 is not a good candidate for this route of administration. It also provides motivation for future studies to test a variety of AAV serotypes and promoters to determine their relative usefulness for suprachoroidal gene transfer.

A clinical trial in patients with retinal vein occlusion demonstrated that suprachoroidal injections of triamcinolone acetonide were safe and well tolerated (12). Although the choroid is a very vascular tissue, there was no evidence of any hemorrhages in the choroid or retina. This is reassuring but additional studies are needed to investigate the safety of suprachoroidal gene transfer. In particular, while we did not observe any signs of inflammation, detailed studies to carefully assess for activation of innate and/or adaptive immunity are needed. Preexistent anti–AAV antibodies do not compromise the efficacy of subretinal injection of AAV vectors, but reduced transgene expression after intravitreous AAV vector injections has been reported (6, 30, 31). This suggests that the subretinal space has greater immune privilege than the vitreous cavity. There is no reason to suspect that the suprachoroidal space would have more immune privilege than the vitreous cavity, and therefore patients without preexistent neutralizing anti–AAV8 antibodies, roughly 50% of the adult population (32), would be the most appropriate patients for initial studies. If it is ultimately determined that preexistent anti–AAV8 antibodies preclude this mode of administration, suprachoroidal injection would still be valuable, because 50% of patients with retinal or choroidal vascular diseases is a large population who could opt for a less invasive procedure that is administered in an outpatient clinic. The ideal target population for suprachoroidal gene therapy for inherited retinal degenerations is young patients with a well-documented pathogenic mutation who have not yet had substantial rod photoreceptor degeneration. Such patients would be less likely to have anti–AAV8 antibodies and suprachoroidal AAV8 gene therapy in both eyes on the same day in an outpatient setting would be an appealing approach.

Intravitreous injections, like suprachoroidal injections, are relatively noninvasive and can be done in an outpatient setting. Transgene expression is limited after intravitreous injection of AAV2, AAV8, or other WT AAV vectors for which it has been tested, because the internal limiting membrane (ILM) provides a physical barrier that binds AAV vectors. Vitrectomy and removal of a portion of the ILM can greatly increase AAV gene delivery from the vitreous cavity, but this is an invasive procedure done in the operating room that shares many complications with subretinal vector injection, although it avoids iatrogenic separation of the RPE and photoreceptors (33). Mutant AAV vectors, in which surface tyrosine residues involved in ubiquitination are replaced with phenylalanines, reduce vector degradation and increase transgene expression at lower vector doses, increasing effectiveness of small amounts of vector that penetrate the ILM (34, 35). Creation of diverse mutant AAV vector libraries and in vivo selection protocols has resulted in identification of vectors that may provide more

extensive infection of retinal cells after intravitreous injection in primates, which may be useful in the future (36).

In summary, suprachoroidal AAV8-mediated gene transfer results in widespread transgene expression throughout the RPE and photoreceptors in rats, nonhuman primates, and pigs, and could lead to a noninvasive outpatient procedure for the treatment of retinal diseases. It avoids vitrectomy and separation of photoreceptors from RPE, which is a major advantage over subretinal vector injections. Transgene expression from a single suprachoroidal injection is comparable to that seen with subretinal injection of the same vector dose, and can be increased by multiple suprachoroidal vector injections. It is currently unknown if this route will be able to replace subretinal injections in patients with preexistent immunity to AAV8, but in many patients it may offer a noninvasive approach to ocular gene transfer that can be done in an outpatient setting.

Methods

Study design. The study was designed to test the level and location of expression of a reporter gene packaged in AAV8 and delivered by suprachoroidal injection. In the second part of the study a comparison was made between suprachoroidal injection and subretinal injection (current favored approach) of AAV8.antiVEGFfab with regard to suppression of VEGF-induced vascular leakage and level of expression.

Preparation of RGX-314 vector. RGX-314 is an AAV8 vector containing a CB7 promoter (chicken β-actin promoter and CMV enhancer), a chicken β-actin intron, a rabbit β-globin poly A signal, and a gene cassette that encodes a humanized monoclonal antigen–binding fragment that neutralizes human VEGF (13). It was produced by triple transfection of adherent HEK293 cells as previously described (37). After harvest, the vector was purified by a 2-step chromatographic step purification methodology (affinity/ion exchange) with subsequent buffer exchange via tangential flow filtration (TFF) into PBS-based formulation buffer. AAV vector genome was titered by digital droplet PCR (ddPCR, Bio-Rad Droplet Digital PCR System QX200) of DNase-resistant particles using primers and probes directed against the polyA sequence encoded in the transgene cassette (38). RGX-314 genomic copy number was 4.0×10^{10} GCs/mL.

Preparation of AAV8-GFP and AAV9-GFP vector. AAV8.CB7.GFP and AAV9.CB7.GFP utilize the same expression cassette as AAV8.antiVEGFfab to express GFP. They were produced by triple transfection of suspension HEK293 cells and purified by a 2-step chromatographic step with subsequent buffer exchange via TFF into PBS-based formulation buffer. Genomic copy number was measured as 9.5×10^{12} GCs/mL by digital droplet PCR. AAV2.CMV.GFP was obtained from Vector Biolabs (catalog 7004).

Animals. All animals were treated in accordance with the Association for Research in Vision and Ophthalmology Statement for Use of Animals in Ophthalmic and Vision Research, and protocols were reviewed and approved by the Johns Hopkins University Animal Care and Use Committee. Norway Brown rats were purchased from Charles River. Adult normal-sighted Rhesus macaques were housed and cared for at the animal facility at the Johns Hopkins University. A 1-month-old (12 kg) Yorkshire pig was purchased from Archway Farms.

Suprachoroidal injection of vector in rats, monkeys, and pigs. Rats were anesthetized with ketamine/xylazine, and eyes were visualized with a Zeiss Stereo Dissecting Microscope. A 30-gauge needle on 1 mL syringe was used to generate a partial thickness (four-fifths through sclera) circumferential opening in the sclera 1 mm posterior to the limbus, and a 34-gauge needle with a blunt 45 degree bevel connected to a 5 μL Hamilton syringe (Hamilton Company) containing vector was inserted into the scleral opening with the bevel facing downward and slowly advanced through the remaining scleral fibers into the suprachoroidal space. The plunger of the syringe was slowly advanced to expand the suprachoroidal space and inject 3 μL containing 1.2×10^8 GCs of AAV8.antiVEGFfab, 2.85×10^{10} GCs of AAV8.GFP or AAV9.GFP, or 2.0×10^{10} GCs of AAV2.GFP vector and held in place for 30 seconds, after which the needle was withdrawn while holding a cotton tipped applicator over the injection site. Visualization of the fundus showed a shallow choroidal detachment on the side of the injection. Antibiotic ointment (Moore Medical LLC) was applied to the ocular surface and rats were returned to their cages.

Three adult Rhesus macaques and one Yorkshire pig were sedated with ketamine hydrochloride (15–20 mg/kg) followed by topical anesthesia of both eyes using 0.5% proparacaine (Akorn) and a drop of 5% povidone iodine. A lid speculum was inserted and the eye was visualized with a Zeiss surgical microscope. A 27-gauge needle attached to an insulin syringe containing the vector was inserted tangentially through the sclera 6 mm behind the limbus. The needle was slowly advanced 4 mm with gentle pressure on the plunger. There was release of resistance when the suprachoroidal space was entered and 50 μL of vector was slowly injected. After 30 seconds, the needle was withdrawn while holding a cotton tipped applicator over the injection site and antibiotic ointment was administered to the ocular surface. The procedure was then repeated for the fellow eye and monkeys were returned to their cages.

Subretinal injection of vector in rats. Rats were anesthetized, pupils dilated, and eyes were visualized with a Zeiss surgical microscope and a 20D Fundus Laser Lens (Ocular Instruments Inc.). A 30-gauge needle on a 1-mL syringe was used to generate a partial thickness circumferential opening in the sclera 1 mm posterior to the limbus. A 34-gauge needle with a blunt 45 degree bevel connected to a 5 μL Hamilton syringe containing vector was inserted into the scleral opening and advanced into the vitreous cavity. While observing the fundus with the 20D lens, the needle was advanced and positioned immediately above the posterior retina. An assistant pushed the plunger to initiate a stream of vector that penetrated the retina, creating a 3 μL bleb. The needle was withdrawn while holding a cotton tipped applicator over the injection site. Antibiotic ointment (Moore Medical LLC) was applied to the ocular surface and rats were returned to their cages.

Tissue harvesting and histology. Rats or monkeys were euthanized and eyes were removed and fixed in 4% paraformaldehyde. Eyes used for flat mounts had the anterior segment and vitreous removed and then retina and RPE/choroid were isolated and flat mounted separately. Eyes for ocular sections were frozen in optimal cutting temperature medium (Thermo Fisher Scientific) and 10-μm frozen sections were placed on slides. Sections were stained with anti-GFP antibody (A21312, Life Technologies Corporation) and Hoechst (Vector Laboratories). Both flat mount and ocular sections were examined by fluorescence microscopy.

The pig was euthanized and eyes immediately removed and placed in 4% paraformaldehyde in 0.1M phosphate buffer, pH 7.4 containing 5% sucrose on ice. After 30 minutes, the corneas were removed and the eyes were incubated in fixative solution at 4°C

overnight. The following day, the eyes were rinsed twice in cool 0.1M phosphate buffer containing 20% sucrose, the lens was removed, and the eyecup was incubated in 0.1M phosphate buffer containing 20% sucrose overnight at 4°C. The eyecups were then washed with fresh sucrose-containing buffer, completely immersed in optimal cutting temperature medium, and frozen. Frozen sections (10 μm) were immunohistochemically stained with anti-GFP antibody and by fluorescence microscopy.

Measurement of GFP protein in retinal or RPE/choroid homogenates. Rat retinal and eyecup samples were isolated under a dissection microscope and put in RIPA buffer (Sigma-Aldrich) containing protease inhibitor cocktail (Roche). Samples were sonicated for 4–5 seconds (Sonic Dismembrator Model 300, Thermo Fisher Scientific), cooled in an ice bath for 5 minutes, centrifuged for 10 minutes at 18,600*g*, and supernatants were stored at –80°C. Total protein concentration was measured using a Bradford CCB-G250 protein-binding assay. Briefly, concentrations of bovine serum albumin (Millipore Sigma) ranging from 20–140 μg/mL were used as standards. A quantity of 25 μL sample or standard was added to duplicate wells of 96-well plates followed by 125 μL Protein Assay Dye (diluted 1:5, Bio-Rad). After a 5-minute incubation on a shaker, absorption was measured at 595 nm in a Spectra Max Plus 384 Microplate Reader (Molecular Devices).

GFP protein levels were measured using a GFP SimpleStep ELISA kit (ab171581, Abcam). Briefly, 50 μL sample or GFP standard dilutions was added to duplicate wells of 96-well plates, followed by 50 μL anti-GFP antibody cocktail. Plates were incubated at 25°C for 1 hour, washed 5 times with rinse buffer, and after addition of 100 μL TMB substrate solution, they were incubated at 25°C in the dark for 10 minutes. After addition of 100 μL stop solution, absorption was measured at 450 nm with a Spectra Max Plus 384 Microplate Reader.

Measurement of antiVEGFfab in retina and RPE/choroid. AntiVEGFfab is very similar to ranibizumab and is recognized by anti-ranibizumab antibodies . The levels of antiVEGFfab in tissue homogenates was measured using a ranibizumab ELISA kit (catalog 200-880-LUG; Alpha Diagnostic Intl) following the manufacturer's instructions.

Assessment of VEGF-induced retinal vascular changes and vascular leakage. Brown Norway rats ($n = 40$) were given a 3 μl suprachoroidal injection of 1.2×10^8 GCs of AAV8.antiVEGFfab in one eye and 2.85×10^{10} GCs of AAV8.GFP ($n = 32$) or vehicle ($n = 8$) in the fellow eye and a second cohort of 40 rats was given a 3 μL subretinal injection of 1.2×10^8 GCs of AAV8.antiVEGFfab in one eye and 2.85×10^{10} GCs of AAV8.GFP ($n = 32$) or vehicle ($n = 8$) in the fellow eye. At 2 weeks after vector injection, 100 ng $VEGF_{165}$ was injected into the vitreous cavity of each eye of 20 rats from each group. After 24 hours, rats were anesthetized, fundus photographs were obtained with a Micron III Retinal Imaging Microscope (Phoenix Research Laboratories, Inc.), and vitreous samples were collected as previously described (19). A rat albumin ELISA kit (ab108790; Abcam) was used to measure albumin levels in vitreous samples as previously described (19). Rats were euthanized and antiVEGFfab levels were measured in retinal and RPE/choroid homogenates as described above. The other 20 rats in each group were given an intravitreous injection of 100 ng in each eye 7 weeks after vector injection, and after 24 hours fundus photographs were obtained, albumin levels were measured in vitreous, and antiVEGFfab levels were measured in retinal and RPE/choroid homogenates.

Statistics. GraphPad Prism version 6.0 software was used for assessment of data distribution and statistical analysis. Data distribution was measured by Shapiro-Wilk test. The 2-tailed Student's *t* test was used for data sets with a normal distribution and a nonparametric test, the Mann-Whitney *U* test, was used for data sets without a normal distribution. *P* values below 0.05 were considered statistically significant and exact *P* values for significant data points are shown in the figures.

Study approval. All experiments were approved by the Johns Hopkins Medicine animal care and use committee.

Author contributions

KD and JS helped to design experiments, performed the majority of experiments, analyzed data, made figures, and helped to write manuscript, and edited manuscript. ZH, SFH, RLS, MK, VEL, DC, RC, and MZ helped to perform some of the experiments, helped to analyze data, and edited manuscript. SVE, NB, MF, OD helped to design some experiment and edited manuscript. PAC designed experiments, helped to analyzed data, wrote first draft of manuscript, and edited manuscript.

Acknowledgments

Funding was provided by REGENXBIO Inc., the Alsheler-Durell Foundation, Per Bang-Jensen, Conrad and Lois Aschenbach, and Andrew and Yvette Marriott.

Address correspondence to: Peter A. Campochiaro, Maumenee 815, The Wilmer Eye Institute, Johns Hopkins Hospital, 600 N. Wolfe Street, Baltimore, Maryland 21287, USA. Phone: 410.955.5106; Email: pcampo@jhmi.edu.

1. Maguire AM, et al. Safety and efficacy of gene transfer for Leber's congenital amaurosis. *N Engl J Med*. 2008;358(21):2240–2248.
2. Bainbridge JW, et al. Effect of gene therapy on visual function in Leber's congenital amaurosis. *N Engl J Med*. 2008;358(21):2231–2239.
3. Hauswirth WW, et al. Treatment of leber congenital amaurosis due to RPE65 mutations by ocular subretinal injection of adeno-associated virus gene vector: short-term results of a phase I trial. *Hum Gene Ther*. 2008;19(10):979–990.
4. Campochiaro PA, et al. Lentiviral vector gene transfer of endostatin/angiostatin for macular degeneration (GEM) Study. *Hum Gene Ther*. 2017;28(1):99–111.
5. Jacobson SG, et al. Improvement and decline in vision with gene therapy in childhood blindness. *N Engl J Med*. 2015;372(20):1920–1926.
6. Bennett J, et al. Safety and durability of effect of contralateral-eye administration of AAV2 gene therapy in patients with childhood-onset blindness caused by RPE65 mutations: a follow-on phase 1 trial. *Lancet*. 2016;388(10045):661–672.
7. Patel SR, Lin AS, Edelhauser HF, Prausnitz MR. Suprachoroidal drug delivery to the back of the eye using hollow microneedles. *Pharm Res*. 2011;28(1):166–176.
8. Patel SR, Berezovsky DE, McCarey BE, Zarnitsyn V, Edelhauser HF, Prausnitz MR. Targeted administration into the suprachoroidal space using a microneedle for drug delivery to the posterior segment of the eye. *Invest Ophthalmol Vis Sci*. 2012;53(8):4433–4441.
9. Patel SR, Berezovsky DE, McCarey BE, Zarnitsyn V, Edelhauser HF, Prausnitz MR. Targeted administration into the suprachoroidal space using a microneedle for drug delivery to the posterior segment of the eye. *Invest Ophthalmol Vis Sci*. 2012;53(8):4433–4441.
10. Chen M, Li X, Liu J, Han Y, Cheng L. Safety and pharmacodynamics of suprachoroidal injection of triamcinolone acetonide as a controlled ocular drug release model. *J Control Release*. 2015;203:109–117.
11. Yeh S, et al. Suprachoroidal injection of tri-

amcinolone acetonide, CLS-TA, for macular edema due to noninfectious uveitis: A randomized, phase 2 Study (Dogwood) [published online ahead of print August 15, 2018]. *Retina (Philadelphia, Pa)*. https://doi.org/10.1097/IAE.0000000000002279.
12. Campochiaro PA, et al. Suprachoroidal triamcinolone acetonide for retinal vein occlusion: results of the Tanzanite study. *Ophthalmol Retina*. 2018;2(4):320–328.
13. Liu Y, et al. AAV8-antiVEGFfab ocular gene transfer for neovascular age-related macular degeneration. *Mol Ther*. 2018;26(2):542–549.
14. Vinores SA, Gadegbeku C, Campochiaro PA, Green WR. Immunohistochemical localization of blood-retinal barrier breakdown in human diabetics. *Am J Pathol*. 1989;134(2):231–235.
15. Vinores SA, Campochiaro PA, Lee A, McGehee R, Gadegbeku C, Green WR. Localization of blood-retinal barrier breakdown in human pathologic specimens by immunohistochemical staining for albumin. *Lab Invest*. 1990;62(6):742–750.
16. Vinores SA, McGehee R, Lee A, Gadegbeku C, Campochiaro PA. Ultrastructural localization of blood-retinal barrier breakdown in diabetic and galactosemic rats. *J Histochem Cytochem*. 1990;38(9):1341–1352.
17. Vinores SA, Amin A, Derevjanik NL, Green WR, Campochiaro PA. Immunohistochemical localization of blood-retinal barrier breakdown sites associated with post-surgical macular oedema. *Histochem J*. 1994;26(8):655–665.
18. Vinores SA, et al. Blood-retinal barrier breakdown in retinitis pigmentosa: light and electron microscopic immunolocalization. *Histol Histopathol*. 1995;10(4):913–923.
19. Fortmann SD, Lorenc VE, Shen J, Hackett SF, Campochiaro PA. Mousetap, a novel technique to collect uncontaminated vitreous or aqueous and expand usefulness of mouse models. *Sci Rep*. 2018;8(1):6371.
20. Thounaojam MC, et al. Protective effects of agonists of growth hormone-releasing hormone (GHRH) in early experimental diabetic retinopathy. *Proc Natl Acad Sci U S A*. 2017;114(50):13248–13253.
21. MacLaren RE, et al. Retinal gene therapy in patients with choroideremia: initial findings from a phase 1/2 clinical trial. *Lancet*. 2014;383(9923):1129–1137.
22. Campochiaro PA, et al. Adenoviral vector-delivered pigment epithelium-derived factor for neovascular age-related macular degeneration: results of a phase I clinical trial. *Hum Gene Ther*. 2006;17(2):167–176.
23. Heier JS, et al. Intravitreous injection of AAV2-sFLT01 in patients with advanced neovascular age-related macular degeneration: a phase 1, open-label trial. *Lancet*. 2017;390(10089):50–61.
24. Igarashi T, Miyake K, Asakawa N, Miyake N, Shimada T, Takahashi H. Direct comparison of administration routes for AAV8-mediated ocular gene therapy. *Curr Eye Res*. 2013;38(5):569–577.
25. Peden MC, et al. Ab-externo AAV-mediated gene delivery to the suprachoroidal space using a 250 micron flexible microcatheter. *PLoS One*. 2011;6(2):e17140.
26. Campochiaro PA, Aiello LP, Rosenfeld PJ. Anti-vascular endothelial growth factor agents in the treatment of retinal disease: from bench to bedside. *Ophthalmology*. 2016;123(10S):S78–S88.
27. Holz FG, et al. Multi-country real-life experience of anti-vascular endothelial growth factor therapy for wet age-related macular degeneration. *Br J Ophthalmol*. 2015;99(2):220–226.
28. Cohen SY, et al. Changes in visual acuity in patients with wet age-related macular degeneration treated with intravitreal ranibizumab in daily clinical practice: the LUMIERE study. *Retina (Philadelphia, Pa)*. 2013;33(3):474–481.
29. Finger RP, Wiedemann P, Blumhagen F, Pohl K, Holz FG. Treatment patterns, visual acuity and quality-of-life outcomes of the WAVE study - a noninterventional study of ranibizumab treatment for neovascular age-related macular degeneration in Germany. *Acta Ophthalmol*. 2013;91(6):540–546.
30. Li Q, et al. Intraocular route of AAV2 vector administration defines humoral immune response and therapeutic potential. *Mol Vis*. 2008;14:1760–1769.
31. Kotterman MA, Yin L, Strazzeri JM, Flannery JG, Merigan WH, Schaffer DV. Antibody neutralization poses a barrier to intravitreal adeno-associated viral vector gene delivery to non-human primates. *Gene Ther*. 2015;22(2):116–126.
32. Calcedo R, Vandenberghe LH, Gao G, Lin J, Wilson JM. Worldwide epidemiology of neutralizing antibodies to adeno-associated viruses. *J Infect Dis*. 2009;199(3):381–390.
33. Takahashi K, et al. Improved intravitreal AAV-mediated inner retinal gene transduction after surgical internal limiting membrane peeling in cynomolgus monkeys. *Mol Ther*. 2017;25(1):296–302.
34. Zhong L, et al. Next generation of adeno-associated virus 2 vectors: point mutations in tyrosines lead to high-efficiency transduction at lower doses. *Proc Natl Acad Sci U S A*. 2008;105(22):7827–7832.
35. Mowat FM, et al. Tyrosine capsid-mutant AAV vectors for gene delivery to the canine retina from a subretinal or intravitreal approach. *Gene Ther*. 2014;21(1):96–105.
36. Santiago-Ortiz J, et al. AAV ancestral reconstruction library enables selection of broadly infectious viral variants. *Gene Ther*. 2015;22(12):934–946.
37. Lock M, et al. Rapid, simple, and versatile manufacturing of recombinant adeno-associated viral vectors at scale. *Hum Gene Ther*. 2010;21(10):1259–1271.
38. Lock M, Alvira MR, Chen SJ, Wilson JM. Absolute determination of single-stranded and self-complementary adeno-associated viral vector genome titers by droplet digital PCR. *Hum Gene Ther Methods*. 2014;25(2):115–125.